2014

Integrating mitosis, toxicity, and transgene expression in a telecommunications packet-switched network model of lipoplex-mediated gene delivery

Timothy M. Martin
University of Nebraska-Lincoln, timothy.michael.martin@gmail.com

Beata Wysocki
University of Nebraska-Lincoln, bwysocki2@unl.edu

Jared P. Beyersdorf
University of Nebraska-Lincoln

Tadeusz A. Wysocki
University of Nebraska-Lincoln, wysocki@uow.edu.au

Angela K. Pannier
University of Nebraska-Lincoln, apannier2@unl.edu

Published in *Biotechnology and Bioengineering* 111:8 (2014), pp. 1659–1671; doi: 10.1002/bit.25207

Submitted September 4, 2013; revised November 27, 2013; accepted January 31, 2014; published online February 21, 2014

Integrating mitosis, toxicity, and transgene expression in a telecommunications packet-switched network model of lipoplex-mediated gene delivery

Timothy M. Martin,[1] Beata J. Wysocki,[2] Jared P. Beyersdorf,[1]
Tadeusz A. Wysocki,[2] and Angela K. Pannier[1]

1. Department of Biological Systems Engineering, University of Nebraska-Lincoln
2. Department of Computer & Electronics Engineering, University of Nebraska-Lincoln

Corresponding author - A. K. Pannier, email apannier2@unl.edu

Abstract
Gene delivery systems transport exogenous genetic information to cells or biological systems with the potential to directly alter endogenous gene expression and behavior with applications in functional genomics, tissue engineering, medical devices, and gene therapy. Nonviral systems offer advantages over viral systems because of their low immunogenicity, inexpensive synthesis, and easy modification but suffer from lower transfection levels. The representation of gene transfer using models offers perspective and interpretation of complex cellular mechanisms, including nonviral gene delivery where exact mechanisms are unknown. Here, we introduce a novel telecommunications model of the nonviral gene delivery process in which the delivery of the gene to a cell is synonymous with delivery of a packet of information to a destination computer within a packet-switched computer network. Such a model uses nodes and layers to simplify the complexity of modeling the transfection process and to overcome several challenges of existing models. These challenges include a limited scope and limited time frame, which often does not incorporate biological effects known to affect transfection. The telecommunication model was constructed in MATLAB to model lipoplex delivery of the gene encoding the green fluorescent protein to HeLa cells. Mitosis and toxicity events were included in the model resulting in simulation outputs of nuclear internalization and transfection efficiency that correlated with experimental data. A priori predictions based on model sensitivity analysis suggest that increasing endosomal escape and decreasing lysosomal degradation, protein degradation, and GFP-induced toxicity can improve transfection efficiency by threefold. Application of the telecommunications model to nonviral gene delivery offers insight into the development of new gene delivery systems with therapeutically relevant transfection levels.

Keywords: nonviral gene delivery, transfection, HeLa, telecommunication modeling, nuclear plasmids, packet-switched network

Introduction

Gene delivery systems use a carrier to transport exogenous genes as plasmid DNA (pDNA) to cells to produce an encoded protein, with the ultimate goal of altering endogenous gene expression and cell behavior with applications in functional genomics (Pannier et al., 2007), tissue engineering (Lu et al., 2013), medical devices (Zilberman et al., 2010), and gene therapy (Niidome and Huang, 2002). While nonviral gene delivery techniques are less efficient than viral systems (Smith and Helenius, 2004), they are considered an attractive alternative because of low toxicity and immunogenicity, lack of pathogenicity, inexpensive synthesis, and easy modification (Boussif et al., 1995; Fasbender et al., 1997; He et al., 2010; Lv et al., 2006). Because of these advantages, empirical investigations into enhancing transfection of nonviral systems continue by means of modifying the pDNA carrier (Guo and Huang, 2012). However, those studies have had limited success in enhancing transfection largely due to the paucity of information on predicting relationships or interactions between parameters

of the delivery agents and the putative barriers to gene transfer (Azzam and Domb, 2004; Baker, 2004; Hagstrom, 2000; Khalil et al., 2006; Medina-Kauwe et al., 2005; Muller et al., 2007; Nishikawa and Huang, 2001; Wiethoff and Middaugh, 2003).

While the exact mechanisms of the transfection process are not fully understood, mathematical and computational models have been developed to provide insight into the process. For example, several pharmacokinetic studies have been instrumental in the development of computational models to describe and predict intracellular behavior of the pDNA during transfection (Dinh et al., 2007; Hakamada and Miyake, 2012; Hume, 2000; Moroianu et al., 1996; Schwake et al., 2010; Varga et al., 2001, 2005; Zelphati and Szoka, 1996). Such models include quantitative structure–activity relationships between vectors and transfection efficiency (Horobin and Weissig, 2005), kinetic models (Banks et al., 2003; Moriguchi et al., 2008; Roth and Sundaram, 2004; Varga et al., 2001, 2005), stochastic stimulations (Dinh et al., 2007), or mechanistic modeling of transgene expression (Berraondo et al., 2009). However, previous models that oversimplify the complexity of gene delivery by compartmentalization (Banks et al., 2003; Ledley and Ledley, 1994) or do not describe the entire transfection process (from internalization of gene to transgene expression) (Parra-Guillen et al., 2010) may lead to information loss or misinterpretation of results. For instance, many models partially describe nonviral gene delivery but biological effects such as mitosis and toxicity, which greatly affect transfection, are not considered (Brunner et al., 2000; Hakamada and Miyake, 2012; Lappalainen et al., 1997; Li et al., 2004). Biological effects such as mitosis and toxicity are often not incorporated into existing models of gene delivery because those effects are generally observed within a time frame beyond that which is described by existing models (Banks et al., 2003; Varga et al., 2001, 2005). However, Jandt et al. (2011) have recently developed a spatiotemporal model that includes mitosis and partitioning of the pDNA content to daughter cells; the model was able to recapitulate the in vitro experiments during a 48 h time frame for plasmid content in the cell nucleus. That model reinforces the need to incorporate biological effects into models of nonviral gene delivery, especially on time frames more relevant to in vitro experiments. However, that model did not describe transgene production or incorporate toxicity. Therefore, new models that can overcome the challenges of reconciling the entire transfection process while accounting for biologically relevant cellular processes are needed in order to provide insight into the design of therapeutically relevant transfection systems.

We have recently described the development of a new type of nonviral gene delivery model using telecommunications theory (Wysocki et al., 2013), presenting an alternative modeling technique to open new perspectives and propose possible pathways for systematic improvement of nonviral gene delivery. The telecommunications modeling technique has been used to describe other intricate "distribution systems," such as data communication networks (Neuts et al., 1970), servicing of patients at hospitals (Kendall, 1953), and, more recently, the HIV infection process (Sharp et al., 2012), a process with many analogues to nonviral gene delivery.

Here, we build on our telecommunication model of gene delivery, where delivery of pDNA to the cell nucleus is considered in the same way as delivery of a packet of information (pDNA) to a destination computer (nucleus) within a random, packet-switched computer network (cell) where the intermediate nodes (barriers to pDNA transfer) decide randomly to which of the outgoing links the incoming packet should be sent (Neuts et al., 1970). In our model, we represent nonviral gene delivery as a digital process, since the events of pDNA transfer occur in terms of integers (e.g., complexes internalized, pDNA internalized into nucleus, transcription from pDNA, etc.). Based on control theory and systems engineering, such digital systems that contain a small number of signals (e.g., plasmids, complexes, mRNA, proteins) are better described using digital modeling techniques compared to modeling using differential equations (Ziemer et al., 1998). Also, in our model, we represent nonviral gene delivery as a stochastic and random process, where routing of the pDNA is random but with probabilities that are influenced by the surrounding conditions. The same routing is described by random packet-switched computer networks, where the packet routing decision can be supported by the information about the current state of the network or packet characteristics (Stallings, 2007). Therefore, since nonviral gene delivery acts a digital and random process, the system can be considered a "queue," and therefore modeled using the well-established queuing theory modeling techniques (Kendall, 1953). Our model describes the transfection process (from internalization to protein folding) over a period of days while simultaneously considering mitosis and toxicity, which are important cellular processes known to occur within that time frame and to affect transfection (Lappalainen et al., 1997; Li et al., 2004). The telecommunication model was constructed in MATLAB by integrating pharmacokinetic parameters from literature with quantitative in vitro experiments. We then compare the telecommunication model in silico output to in vitro results for lipoplex-mediated delivery of pDNA encoding the enhanced green fluorescent protein (eGFP) gene to HeLa cells. A priori predictions based on sensitivity analysis suggest possible improvements to the lipoplex gene delivery system to guide designs of therapeutically relevant transfection systems.

Theoretical Aspects

To develop the novel model of DNA transfer, the nonviral delivery process was first abstracted as a packet-switched network. That telecommunication network was then implemented in MATLAB as a model by applying queuing theory to describe the arrival and departure of information throughout the network. Finally,

because biological processes are highly parallel, the queue reduces the nonviral gene delivery abstraction to a pharmacokinetic model that is: (1) Poisson distributed to account for discrete (i.e., integer) numbers of packets, (2) a Markov process, in that the current state of the packets in the system will affect the current iteration of the simulation, (3) random distributed, in that probabilities based on the pharmacokinetic values dictate routing, and (4) stochastic as noise is added to each pharmacokinetic parameter during each iteration. Therefore, we model nonviral gene delivery as a discrete and stochastic process, unlike existing models that may be continuous and/or deterministic (Banks et al., 2003; Brunner et al., 2000; Hakamada and Miyake, 2012; Lappalainen et al., 1997; Ledley and Ledley, 1994; Li et al., 2004; Parra-Guillen et al., 2010; Varga et al., 2001, 2005).

Packet-Switched Network

The process of nonviral gene delivery was abstracted as a packet-switched network, in which delivery of genetic information to the cell nucleus can be considered in the same way as delivery of a packet of information to the destination computer within a packet-switched network (Figure 1). In such a network, the data packets (i.e., pDNA or its altered form as mRNA or GFP) are transmitted through several intermediary nodes (routing through intermediate barriers) to ensure the packet payloads arrive intact at the destination (transgene product in the post-nuclear cytoplasm). The packets can be transmitted via different routes depending on the state of the nodes in the system and/or packet characteristics (e.g. unpacked/packed state of complex, marking of molecules for degradation, presence of nuclear localization signals (NLSs), and nuclear breakdown). The nodes in this network represent components of the cell that act as servers (i.e., processing or altering of the information occurs) involved in pDNA transfer: milieu, endosome, lysosome, cytoplasm (before nucleus), nucleus, and cytoplasm (after nucleus). Within each node are layers that dictate the processing of information concerning the packet (pDNA, mRNA, GFP): *physical layer* is where movement of the packet occurs, *network layer* is where modification of the packet occurs, which affects routing, *transport layer* controls the packet format (packed/unpacked/marked) and checks integrity (intact/degraded), and the *application layer* uses the pDNA to create the specified functional protein that is encoded within the DNA. Each cell in the in silico experiment consists of such a network. The abstraction of the nonviral gene delivery process in layers is more thoroughly described in our previous work (Wysocki et al., 2013). Queuing theory was then used to implement the network as a model in MATLAB, as described next.

Queuing Theory

The packet-switch network was implemented in MATALB using queuing theory. The pDNA arrival process was assumed to be random at the input of each node, and to follow a Poisson distribution. The Poisson distribution is often used to model events that happen rarely but have very many opportunities to happen (Ross, 2000), which is appropriate for a pDNA delivery system where around 1% of the initially delivered pDNA makes it to the nucleus (Tachibana et al., 2004). The arrival distribution is characterized by a rate parameter λ, with outcomes $\lambda = 1$ for success with probability P, and $\lambda = 0$ for failure with probability $q = 1 - P$, where $0 < P < 1$. The expected value of λ is E(λ)=P Thus, the expected number of successes (i.e., input of one DNA complex, pDNA, mRNA, or GFP into the next active node) in a single service is the probability that the trial will be a success. Therefore, the number of arrivals in any given time interval $(t, t+\tau)$ follows a Poisson distribution with a parameter $(\lambda\tau)$, such that

$$P\left[\left(N(t+\tau) - N(t)\right) = k\right] = \frac{e^{-\lambda\tau}(\lambda\tau)k}{k!} \quad (1)$$

where e is the base of the natural logarithm ($e = 2.71828\ldots$) and $N(t+\tau) - N(t) = k$ is the number of arrivals in the interval $(t, t+\tau)$. The arrival process was modeled as an inhomogeneous Poisson process, with

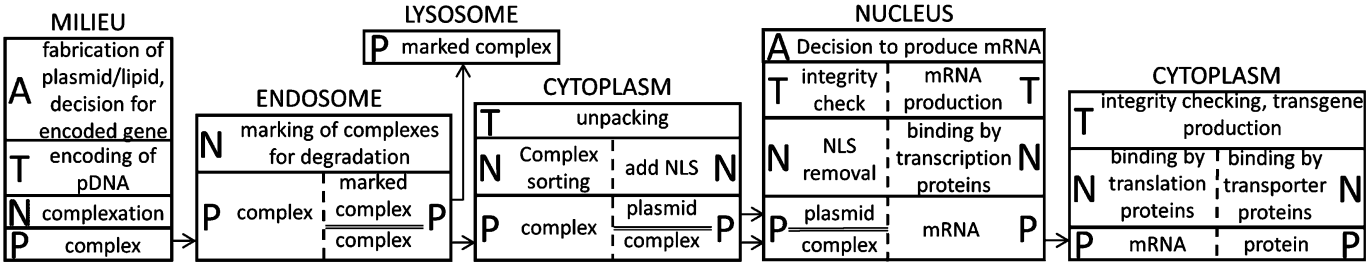

Figure 1. Modeling nonviral gene delivery as a packet-switched network. Each barrier of the gene delivery process is represented by an individual node containing layers, which dictate transmission of the data packet, that is, pDNA transfer (see Theoretical Aspects section). The physical layer (P) is where movement of the packet occurs. The network layer (N) is where modification of the packet occurs, which affects addressing or routing. The transport layer (T) controls the packet format and checks integrity. The application layer (A) uses the information encoded in the delivered packet (complex, pDNA, mRNA, or GFP) to perform a desired operation.

the intensity $\lambda(t)$ being a function of time. In such a process, the expected number of events within a time interval (a, b) is:

$$\lambda_{a,b} = \int_a^b \lambda(t)\, dt \tag{2}$$

and the number of arrivals in that time interval

$$P\left[(N(b) - N(a)) = k\right] = \frac{e^{-\lambda_{a,b}}\, \lambda_{a,b}^{k}}{k!} \qquad k = 0, 1, 2, \ldots \tag{3}$$

The arrival process of the pDNA or complex at each node is also modeled as a Markov process in which the outcome of distributions for the data packets are only dependent on the previous simulated state of the network, and therefore *memoryless* (Ross, 2000).

After arrival of the packet at each node, the pDNA or DNA complex is serviced (i.e., processed) with an exponentially distributed service time, μ, also modeled as a Markov process. The exponential distribution is described by the probability density function:

$$f(x;\mu) = \begin{cases} \mu e^{-\mu x}, & x \geq 0 \\ 0, & x < 0 \end{cases} \tag{4}$$

Biological processes can be considered as highly parallel; therefore the number of customers (DNA complex, pDNA, mRNA, GFP) < servers (nodes), which results in a total departure or instantaneous service rate equal to $(n\mu)$, where n is the number of complexes, pDNAs, mRNAs, or GFPs being serviced (i.e., processed at each node) at each time intervals. Therefore the output from one node and input into the next intermediate node follows a Poisson distribution, where $\lambda(t) = \mu(t)$, allowing the packet-switched network to be represented as a pharmacokinetic model with service rates (i.e., processing at each node) equal to the kinetic constants available in literature (Table I). Since the actual kinetic could be higher or lower than the reported average, $\mu(t)$ was implemented in the model to change randomly around the respective mean values, as 10% standard deviation with Gaussian distribution, thereby creating a stochastic system. When multiple routes for the packet are available, a probabilistic directing of services was used as previously described (Wysocki et al., 2013). The same approach for directing of services was used in a spatiotemporal model of gene delivery (Jandt et al., 2011). Therefore, using queuing theory, the abstracted packet-switched network of the gene delivery process (Figure 1) can be represented as a pharmacokinetic model that is discrete and stochastic (Figure 2; see below).

Pharmacokinetic Model

The nonviral gene delivery process was represented as a reactive system (Fisher and Henzinger, 2007), where each process may change state in reaction to another process changing state (Figure 2). The processes included in this model are internalization, endosomal escape, lysosomal degradation, binding of nuclear import proteins (complexes), unpacking of pDNA from DNA carrier, nuclear pore import (pDNA or complexes), degradation of unpacked pDNA, binding of nuclear import proteins (pDNA), nuclear-area localization during mitosis, nuclear localization, detachment of nuclear import proteins (pDNA or complexes), transcription, mRNA degradation, translation, protein (unfolded) degradation, protein maturation, and protein (folded) degradation. The rates at which these processes occur are identified in the literature (see references in Table I), but distributed as described above. Based on the available first-order kinetics for each process (Table I), the simplest model was developed, in terms of accounting for the key processes in an even more complex DNA transfer process. Such a computational model is well suited to representing a complicated chain of events, even when not every detail about the process is known (Fisher and Henzinger, 2007).

Methods

Computational Model

Queuing theory was used to model the telecommunications packet-switched network in MATLAB (Neuts et al., 1970), as described above. Model simulations were run in ½ second increments while keeping track of subcellular distribution data of the complex, pDNA, mRNA, and protein for each cell in the experiment at each time increment. The averages of the subcellular distribution data of all the cells in the experiment at each time increment was collected as an averaged singleton. For sensitivity analyses, main effect sensitivity S_j for the model of k inputs to transfection output of $y = f(\mu_1, \mu_2, \ldots, \mu_k)$ was calculated as follows:

$$S_j = \left| \frac{\left(V(Ey \mid \mu_j)\right)}{V(y)} \right| \times \frac{1}{2\,\mu_j^{0.0s'}} \qquad j = 1, 2, \ldots, k \tag{5}$$

where $E(y)$ is the expected value of y, $V(y)$ is the variance of the model output y, and $V(E(y \mid \mu_j)$ is the variance of the expected value of y conditional on values of input j (Mokhtari et al., 2006). For all in silico simulations, the initial number of cells in the experiment was set to 5,000. For in silico and in vitro experiments lipoplexes were allowed to remain in contact with the cells for 4 h. Within the model, successful transfection is achieved when the number of GFP molecules in a cell reaches three or greater, since the fluorescence from multiple GFP molecules provides a stronger signal than a single GFP (Cinelli et al., 2000) and, therefore, in silico transfection will more closely resemble in vitro transfection measurements using fluorescence cytometry (see below).

Cell Culture and Transfection

HeLa cells (ATCC, Manassas, VA) were cultured in T-75 flasks in Dulbecco's Modified Eagle's Medium

Table I. Summary of kinetic parameters used for model (see Figure 2)

Kinetic parameter description	Rate k (s^{-1})	Reference
μ_1 Internalization	1.45	Calculated from Lipofectamine delivery of pWizβGal under direction of CMV promoter to HEPG2/C3A cells (Varga et al., 2005)
μ_2 Endosomal escape	1.7×10^{-4}	Calculated from ODN release from DOSPA/DOPE lipoplexes (Lappalainen et al., 1997); used to model lipoplex gene delivery (Varga et al., 2001)
μ_3 Lysosomal degradation	3.33×10^{-4}	Reported to be experimentally found and used to model Lipofectamine delivery of pWizβGal to HEPG2 cells (Varga et al., 2005)
μ_4 Attachment of importins (complexes)	1.7×10^{-3}	Estimated from the kinetic parameter from adenoviral vector kinectics which show similar kinetics as lipoplexes until post nuclear events (Varga et al., 2005), consistent with a recent report (Rehman et al., 2013)
μ_5 Unpacking of pDNA	3.5×10^{-3}	Calculated from FRET signal quenching of synthesized unilamellar vehicles added to DOTAP/ODN lipoplexes (Zelphati and Szoka, 1996)
μ_6 Nuclear pore import	5.0×10^{-5}	Reported to be experimentally found and used to model Lipofectamine delivery of pEGFP-C1 to HEPG2 cells (Varga et al., 2001)
μ_7 Degradation of pDNA	8.3×10^{-5}	Calculated by FISH for pGL2 encoding luciferase (Lechardeur et al., 1999); similarly reported elsewhere (Dean et al., 1999) and used to model Lipofectamine delivery of pWizβGal to HEPG2 cells (Varga et al., 2001)
μ_8 Attachment of importins(pDNA)	3.3×10^{-5}	Reported to be found and used to model Lipofectamine delivery of pEGFP-C1 to HEPG2 cells (Varga et al., 2001) and consistent with a report of unpacking of PNA-labeled pDNA in HeLa cells (Wilson et al., 1999).
μ_9 Nuclear-area localization during mitosis	2.8×10^{-4}	Calculated from LF2000 delivery of pCMV-Venus yellow fluorescent protein to HeLa cells using time lapse images (Hakamada and Miyake, 2012).
μ_{10} Nuclear localization	1.7×10^{1}	Reported to be experimentally found and used to model Lipofectamine delivery of pWizβGal to HEPG2 cells (Varga et al., 2001).
μ_{11} Detachment of importins	1.7×10^{1}	Reported to be found (Moroianu et al., 1996) and used to model Lipofectamine delivery of pWizβGal to HEPG2 cells (Varga et al., 2001)
μ_{12} Transcription	5.0×10^{-2}	Reported to be experimentally found from time lapse images and theoretical models of GFP expression in BEAS-2B cells transfected with LF2000 (Schwake et al., 2010). The value of this parameter is consistent with other reports (Hume, 2000).
μ_{13} mRNA degradation	2.8×10^{-5}	Calculated from GFP mRNA stability experiments using Northern blot (Sacchetti et al., 2001); also used in theoretical models of GFP expression in BEAS-2B cells transfected with LF2000 (Schwake et al., 2010).
μ_{14} Translation	2.8×10^{-2}	Reported to be found from time lapse images and theoretical models of GFP expression in BEAS-2B cells transfected with LF2000 (Schwake et al., 2010); consistent with other reports in literature (Alberts, 1994)
μ_{15} Protein (unfolded) deg.	1.4×10^{-4}	Reported to be found from time lapse images and theoretical models of GFP expression in BEAS-2B cells (Schwake et al., 2010)
μ_{16} Protein maturation	2.8×10^{-4}	Calculated from time for chromophore formation in presence of inclusion bodies (Sniegowski et al., 2005). The value of this parameter was also used in theoretical models (Schwake et al., 2010).
μ_{17} Protein (matured) degradation	3.6×10^{-6}	Calculated from GFP protein stability experiments using Western blot (Sacchetti et al., 2001). A similar value for this parameter was also used in theoretical models (Schwake et al., 2010).

The parameter values are first-order rate constants and therefore have units of s^{-1}. CMV, cytomegalovirus; DDAB, monocationic dimethyl-dioctadecylammonium bromide; DOPE, dioleoyl-phosphatidylethanolamine; DOSPA, polycationic 2,3-dioleoyloxy-N-[2(sperminecarboxamido)ethyl]-N,N-dimethyl -1-propanaminium trifluoroacetate; LF2000, Lipofectamine®2000; ODN, oligodeoxynucleotide.

(DMEM, Gibco/Invitrogen, Carlsbad, CA) containing 4.5 g/L glucose, supplemented with 10% fetal bovine serum (Gibco), 2 mM L-glutamine (Gibco), and 100 units/mL of penicillin/streptomycin (Gibco) and maintained at 37°C in a humidified 5% CO_2 atmosphere. Cells were dissociated at confluence with 0.05% Trypsin-EDTA and viable cells were counted using a hemocytometer and trypan blue dye exclusion assay. Cells were seeded at a density of 28,000 cells/cm^2 for flow cytometric analysis and WST-1 assays (in 300 µL into wells of a 48-well plate; see below) and for nuclei isolation (in 10 mL into T-75 flasks; see below). After cell adherence (~18 h after cell seeding), lipoplexes were formed and delivered to the cells at a volume of 100 µL/cm^2 and a dose of 0.27 µg/cm^2. Plasmid pEGFPLuc, which encodes for both the eGFP and firefly luciferase protein (LUC) under the direction of a CMV promoter (Clontech, Mountain View, CA) was used for all transfection experiments. Plasmids were purified from bacteria culture using Qiagen (Valencia, CA) reagents and stored in Tris–EDTA buffer solution (10 mmol/L Tris, 1 mmol/L EDTA, pH 7.4) at −20°C. Lipoplexes were formed with Lipofectamine 2000 (LF2000; Invitrogen), following manufacturer's instructions. Briefly, DNA complexes were formed at a pDNA: lipid ratio of 1:1.3 (w/v) in serum-free OptiMEM media (Invitrogen) by adding transfection reagent diluted in media dropwise to pDNA diluted in media, mixing by gentle pipetting, and incubating for 20 min. Lipoplexes were allowed to remain in contact with the cells for 4 h, and then the media was aspirated, cells were rinsed once with 1× PBS, and fresh medium added to the cells. Control flasks were seeded

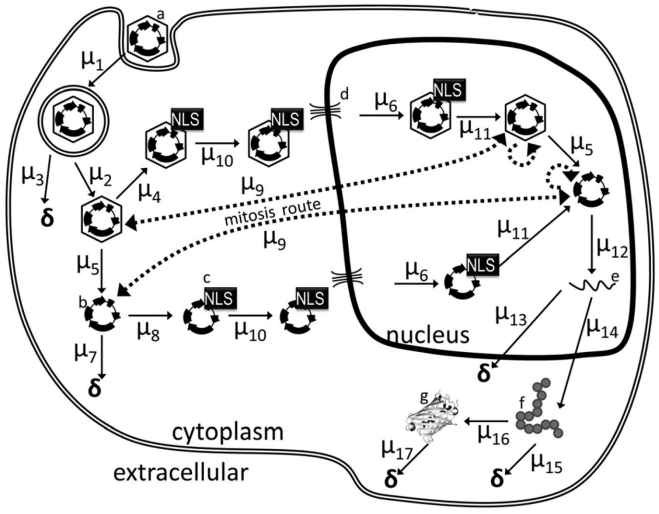

Figure 2. Routing of nonviral complexes. After delivery and arrival to cells, the pDNA will route differently in the packed state, unpacked state, or if the cell is undergoing mitosis. Routes that are active during mitosis are indicated by dashed lines. Kinetic parameters are shown in Table I. Mitosis rate was determined by WST-1 assay (see Supplementary Figure S1 and Methods section). [a]packed plasmid; [b]unpacked plasmid; [c]nuclear import binding proteins; [d]nuclear pore complex; [e]mRNA; [f]unfolded protein; [g]folded protein; δ indicates degradation.

as described above, without the addition of lipoplexes. Cells were then assayed for proliferation, toxicity, transfection efficiency, and nuclear plasmids (see sections below).

WST-1 Cell Proliferation and Toxicity

Cells were seeded and transfected as described above. Medium was removed, cells were rinsed with 200 μL 1× PBS, and 200 μL WST-1 solution (WST-1 reagent [Clontech] diluted 1:9 in phenol-free DMEM [Gibco]) was added to cells at 5, 13, 21, and 45 h post-delivery of the lipoplexes (treated) or without lipoplexes (control). Three hours after addition of WST-1 solution, absorbance measurements were taken at 430 nm (reference 690 nm; background adjusted to WST-1 solution-only wells). An $n=6$ was used for treated conditions and $n=3$ was used for control conditions.

Transfection Efficiency and Flow Cytometric Analysis

Cells were seeded and transfected as described above. Transfection efficiencies were assayed at 8, 16, 24, and 48 h post-delivery of the lipoplexes using fluorescence activated cell sorting (FACS). At each time point indicated, cells were dissociated with the addition of 0.05% Trypsin-EDTA, followed by inactivation of enzyme with addition of an equal volume of completed media, and then three wells of a 48-well plate were pooled and placed on ice for a single sample, $n=1$. Flow cytometric analysis was performed using a Cytek DxP10 cell counter (University of Nebraska-Lincoln's Center for Biotechnology Flow Cytometry Core Facility), with detection of GFP with excitation at 488 nm and emission at 530±15 nm. A live gate was set in forward scatter (FSC) versus side scatter (SSC) plot to remove cell debris or clumped cells from the count. The number of GFP positive cells counted was divided by the total cell count (a minimum of 5,000 gated cells counted) and reported as transfection efficiency. Counts from an $n=6$ was collected at each time point.

Nuclei Isolation and Plasmid Quantification

Cells were seeded and transfected as described above. Nuclei were isolated, purified, and the number of pEGFPLuc plasmids per cell nucleus was found at 8, 16, and 24 h post-delivery. Nuclei were isolated from cells in two, pooled T-75 flasks using a using an iodixanol gradient, as previously described (Cohen et al., 2009). Nuclei isolation was confirmed by Hoechst stain and fluorescence microscopy (data not shown). Nuclei were lysed with 0.5% sodium dodecyl sulfate and DNA was collected in the aqueous phase by phenol extraction and further purified by collecting the aqueous phase and performing a second extraction with 25:24:1 phenol/chloroform/isoamyl alcohol (Thermo-Fisher). After an ethanol precipitation the DNA was suspended in DEPC. Quantification of nuclear plasmids was performed by a previously described method (Cohen et al., 2009) using qPCR to determine the number of copies of the plasmid, modified by normalization method in which the number of cells was determined by using the slope obtained for *eGFP* curve to convert CT value obtained for *ACTA1* to copy number. *ACTA1* was assumed to be a single copy gene and to have the same qPCR efficiencies as *eGFP* (Cohen et al., 2009), therefore every two copies of *ACTA1* represent 1 cell in the experiment. Primers (IDT, Skokie, IL) used were *ACTA1* Forward 5′-TCAGAAAGATTCCTACGTGGGCGA-3′, *ACTA1* Reverse 5′-TGTGGTGCCAGATCTTCTCCATGT-3′ and *eGFP* (Hama et al., 2007). An $n=6$ was used for all time points.

Results and Discussion

Initial Model Performance

Development of the model is detailed in the Theoretical Aspects section of this work. After reconciling the reported kinetics (Table I) into the telecommunication model, little difference between in silico and in vitro transfection efficiency is observed early after DNA delivery, with both model and experimental data showing ~20% transfection efficiency 10 h after treatment with complexes (Figure 3A). Previous models have been developed to represent transfection consistent with this time frame and report similar agreement between model output and in vitro results (Banks et al., 2003; Varga et al., 2001). However, our model reported nearly 100% transfection after 48 hours (Figure 3A), a prodigious overestimate of transfection efficiency, which was measured as ~30% after 48 h. The overestimation of

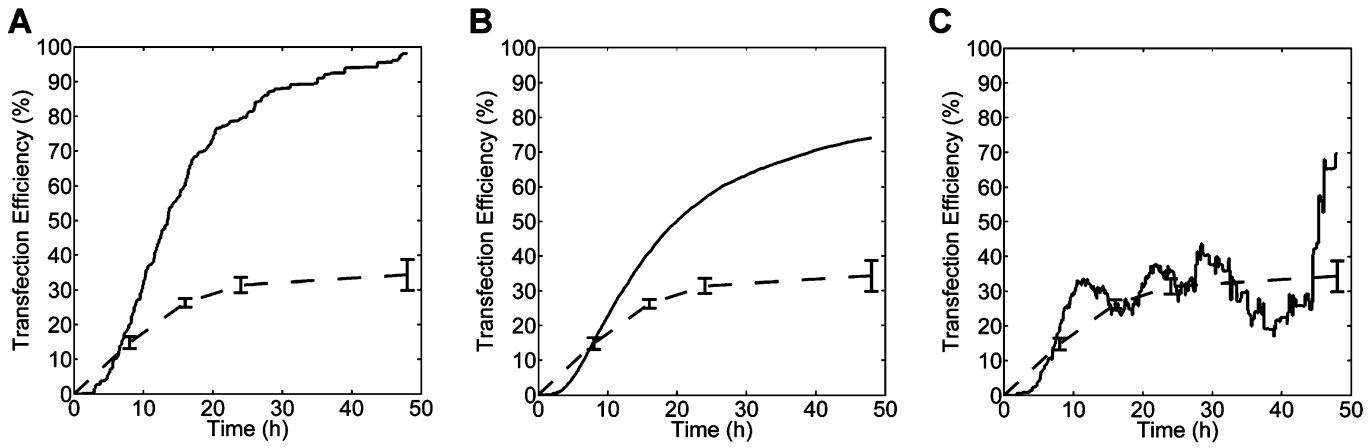

Figure 3. The effects of mitosis and toxicity on transfection. The model was initially compiled accounting only for pharmacokinetic parameters (Table I), without mitosis and without toxicity (**A**). Accounting for only mitosis (**B**) or toxicity (**C**) resulted in reduced transfection levels. The time points on the graph represent model and experimental results after addition of lipoplexes to HeLa cells. Model data, solid line, are reported as mean of output from all simulations (see Methods section). Experimental data, dashed line, are reported as the mean ± SEM ($n = 6$).

transfection by the telecommunication model can likely be attributed to the ability of retransmitting those complexes, pDNAs, or mRNAs that fail to progress past a barrier at an earlier time point, provided degradation has not occurred. Retransmission occurs biologically and is executed easily in a telecommunications computational model (Fisher and Henzinger, 2007), but most models follow deterministic mathematical rules where the algorithm fails to describe retransmit ability (Banks et al., 2003; Parra-Guillen et al., 2010; Varga et al., 2001, 2005). Given the overestimation of transfection with the first version of our telecommunications model, a typical modeling technique would be to undergo a training session to tune the kinetic parameters so in silico and in vitro results agree, followed up with an in vitro validation experiment (Banks et al., 2003; Jandt et al., 2011). However, such an approach should be discouraged because pharmacokinetic parameters should not change, and the overestimate highlights that the model did not account for other biological effects relevant to transfection. Since our model is the first to reconcile the kinetic parameters for all processes and to simulate DNA transfer up to 48 h, we recognized mitosis and toxicity were left unaccounted for in the model, even though their effects are evident in in vitro experiments (Supplementary Figure S1, see below) (Lappalainen et al., 1997) and known to affect transfection (Brunner et al., 2000; Hakamada and Miyake, 2012; Martin et al., 2013). Longer time frames are more representative of time points for in vitro experiments and therefore mitosis and toxicity effects were incorporated into the model and then used for simulations.

Solely Incorporating Mitosis in the Model

Mitosis has been shown in many reports to affect the transfection process (Brunner et al., 2000; Hakamada and Miyake, 2012), but the effect has never been quantified or included in a nonviral gene delivery model. Therefore in vitro experiments using WST-1 proliferation assay were conducted on control cells to determine the mitosis rate of HeLa cells in an in vitro culture system (Supplementary Figure S1). The doubling time for HeLa cells is approximately 18 h and therefore, one would expect a 100% increase in the number of cells in the experiment every 18 h. However, according to the WST-1 cell proliferation assay, we observed an increase in cells in the experiment of approximately 2.3% per hour, or 41.4% every 18 h (Supplementary Figure S1). Possible reasons for the reduced rate of growth are lack of space, lowered nutrient availability, or contact-inhibited growth. Some cells also exhibit growth rate that is dependent on the plasmid copy number inside the cell (Klumpp, 2011). To add these limitations to the model, this measured mitosis rate was used and was scaled accordingly with the mitosis event initially occurring at any random time point within an approximate 18 h time period to recapitulate the in vitro environment for non-synced cells. After a cell underwent mitosis, the next mitosis event, for a random portion of the simulated cells, occurred stochastically with a mean of 18 h. After solely incorporating mitosis without toxicity effects in the model simulations, in silico transfection level agreed with in vitro levels at the 8 h time point, but the model grossly overestimated transfection by 15%, 25%, and 40% at the 16, 24, and 48 h time points, respectively (Figure 3B). The addition of mitosis to the model alone was not enough for the model to accurately predict in vitro transfection levels, but reduced transfection levels compared to the original model (without mitosis and without toxicity) were observed (Figure 3A). Likely contributions to the reduced transfection levels could be dilution of the pDNA and GFP when distributed to daughter cells (Gasiorowski and Dean, 2005; James and Giorgio, 2000; Tachibana et al., 2004; Varga et al., 2001), added exposure of the pDNA to the nucleases during

nuclear breakdown and therefore degradation (Lechardeur et al., 1999), pDNA carrier association with mRNA which may impede translation (Hama et al., 2007), or increase in total number of cells in the experiment and therefore a larger divisor in the calculation. Therefore, including mitosis alone was not enough for the model to accurately predict transfection.

Solely Incorporating Toxicity in the Model

Toxicity or cell stress considerations are important in the design of the delivery system and have been shown to affect transfection (Candiani et al., 2010; Martin et al., 2013; Plautz et al., 2011; Schweikl et al., 2008). Treatment of cells with lipoplexes has been previously reported to result in lower total cell numbers, compared to control (Lappalainen et al., 1997), or cell senescence (Ludtke et al., 2002), but the effect was never quantified nor has it ever been included in a model of nonviral gene delivery. From in vitro transfection experiments in our lab, those cells which exhibit very high GFP fluorescence as observed by Leica DMI 3000B fluorescence microscopy are usually rounded, punctate, or detached indicating treatment-induced necrosis, whereas, those cells with relatively lower GFP intensity do not exhibit treatment-induced necrotic morphology (data not shown). Typically, as the number of lipoplexes increases in the cell, the amount of transgene production increases (i.e., number of GFPs) (Tachibana et al., 2004) in addition to increases in cytotoxicity in a dose-dependent manner (Lv et al., 2006). Simulations from our model agree with those observations (data not shown). Therefore, for the purposes of including toxicity in the model, we have linked cell death to a relative GFP number and the GFP-induced toxicity should be viewed as encompassing all sources of toxicity in the cell, not just due to folded GFP protein in the cell as the name may infer. The toxicity effect on cell growth was determined by assaying lipoplex-treated cells using WST-1 toxicity assay (Supplementary Figure S1), which showed that approximately 1.2% of cells are lost each hour due to treatment-induced toxicity. In order to achieve the same effect in the in silico model, toxicity was incorporated by removing those cells from the simulation with overproduction of GFP in a Bernoulli distributed manner. At each 0.5 s increment of the simulation, an increasing probability of cell death was determined for those cells with greater than 500 GFPs:

$$P_D(n) = \begin{cases} 0, & n \le 500 \\ \operatorname{erf}\left(\dfrac{n-500}{2000}\right), & n > 500 \end{cases} \quad (6)$$

Using that equation, the relative number of GFPs used in silico was able recapitulate the approximately 1.2% loss of cells per hour observed in the in vitro experiment for toxicity (Supplementary Figure S1; data not shown). The reason for reduced cell proliferation after lipoplex treatment is unknown, but protein synthesis is energy-intensive and overproduction of the transgene may lead to a starvation condition in which the cell cannot effectively adapt (Jewett et al., 2009). After solely incorporating toxicity without mitosis effects in model simulations, in silico transfection levels more closely followed in vitro transfection levels at 8, 16, and 24 h time points but the model grossly overestimated transfection by 40% at the 48 h time point (Figure 3C). The observed transfection profile appeared erratic because shortly after a plasmid reaches the nucleus, the GFP transgene is rapidly produced and accumulates to levels that lead to cell death. Therefore, oscillations in transfection are observed because an increase in transfection is shortly followed by death of that transfected cell. Dead cells are not considered in calculations, and as a result, over time the number of cells in the experiment drastically drops and those oscillations appear more drastic after 40 h (Figure 3C). Therefore, including toxicity alone was not enough for the model to accurately predict transfection.

The Effect of Mitosis and Toxicity in the Model on Transfection

When toxicity and mitosis were both added to the model, reported transfection efficiency was approximately 30% after 24 h and was not statistically different than transfection efficiency measured in in vitro experiments (Figure 4A) at any time point. Including mitosis and toxicity in the model had a compound effect in reducing transfection efficiency in model simulations. Additionally, the oscillations observed in simulations from a with-toxicity-without-mitosis model (described above; Figure 3C) are not present when mitosis is also incorporated into the model due to dilution of cellular content from mother cell to daughter cells. These transfection trends reported here for both in silico and in vitro experiments are also similar to transfection efficiencies reported for HeLa cells transfected using DOTAP (1,2-dioleoyloxy-3-trimethylammoniumpropan):DOPE lipoplexes (James and Giorgio, 2000) or TFL-3 lipoplexes (Li et al., 2004). In addition to reporting transfection efficiencies, the number of nuclear-associated plasmids has been correlated to transgene expression (James and Giorgio, 2000); therefore we compared the output of our model, which includes toxicity and mitosis, to experimental data in regards to the number of nuclear pDNAs (Figure 4B), which demonstrated that these numbers were not statistically different between in silico and in vitro experiments. These results agree with other reports showing the peak number of nuclear plasmids to occur at 8 h (~2,000 plasmids/nucleus) and decrease slowly 24 h (~1,200 plasmids/nucleus) after initial delivery of lipoplexes to HeLa cells (Banks et al., 2003; James and Giorgio, 2000; Li et al., 2004). A lag in the peak number of plasmids compared to peak transfection was observed (Figure 4A and B), which is an effect commonly reported for lipoplexes (Banks et al., 2003; Tachibana et al., 2004). Together, the simulation results for toxicity and mitosis potentially highlights the significance of senescence (Ludtke et al., 2002) and GFP-induced necrosis on transfection success (Moriguchi et al., 2008).

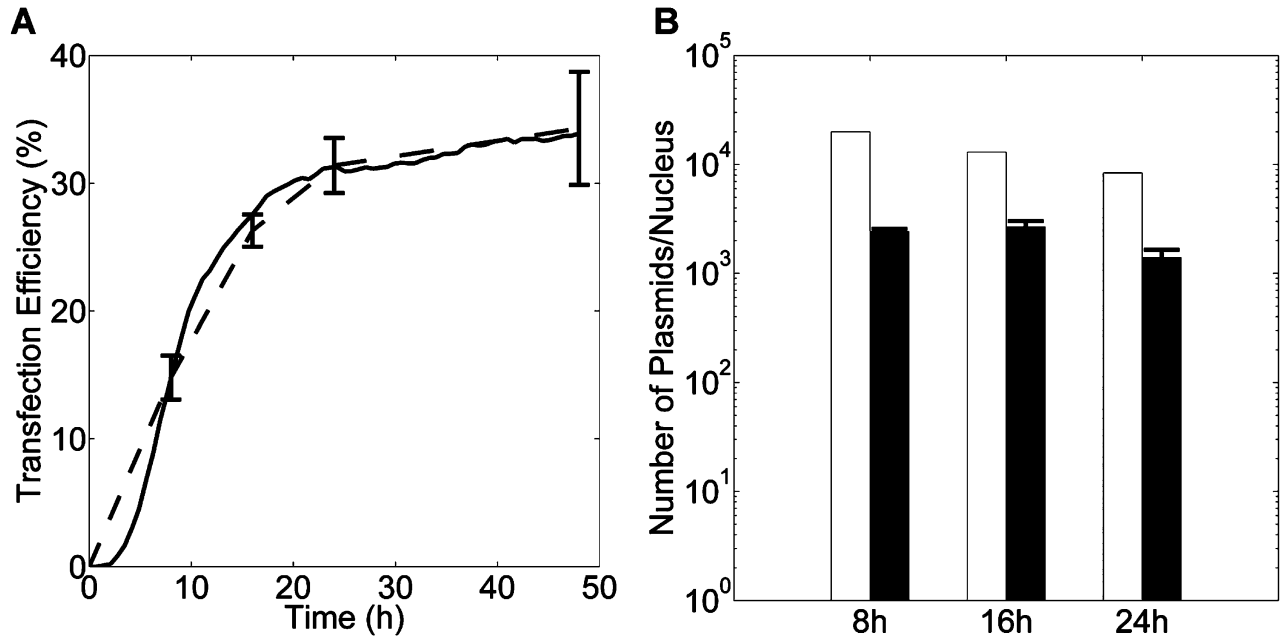

Figure 4. Model agrees with experimental results. The model was modified to include mitosis and toxicity effect and output was compared to in vitro results at the indicated time points after lipoplex delivery to HeLa cells. Transfection efficiency was measured using FACS (**A**) or the number of plasmids per nucleus was quantified using qRT-PCR (**B**). Model data, solid line or white bars, are reported as mean of output from all simulations. Experimental data, dashed line or filled bars, are reported as the mean ± SEM ($n = 6$). Chi-square test confirms no statistical difference between the model and experimental results with an $\alpha = 0.05$.

Toxicity Threshold Effect on Cell Viability and Transfection

Since our new telecommunication model of gene delivery can accurately predict in vitro experiments when mitosis and toxicity are included in the model, we next set out to explore their effect on transfection (Figure 5A and B) by varying the threshold for GFP-induced toxicity (see Methods section). The simulations show that increasing the threshold for toxicity-induced cell death with GFP overproduction results in improved cell viability and increased transfection efficiency from ~30% to ~70%, when the toxicity effect is reduced eightfold from 500 GFPs to 4,000 GFPs (Figure 5A and B). These

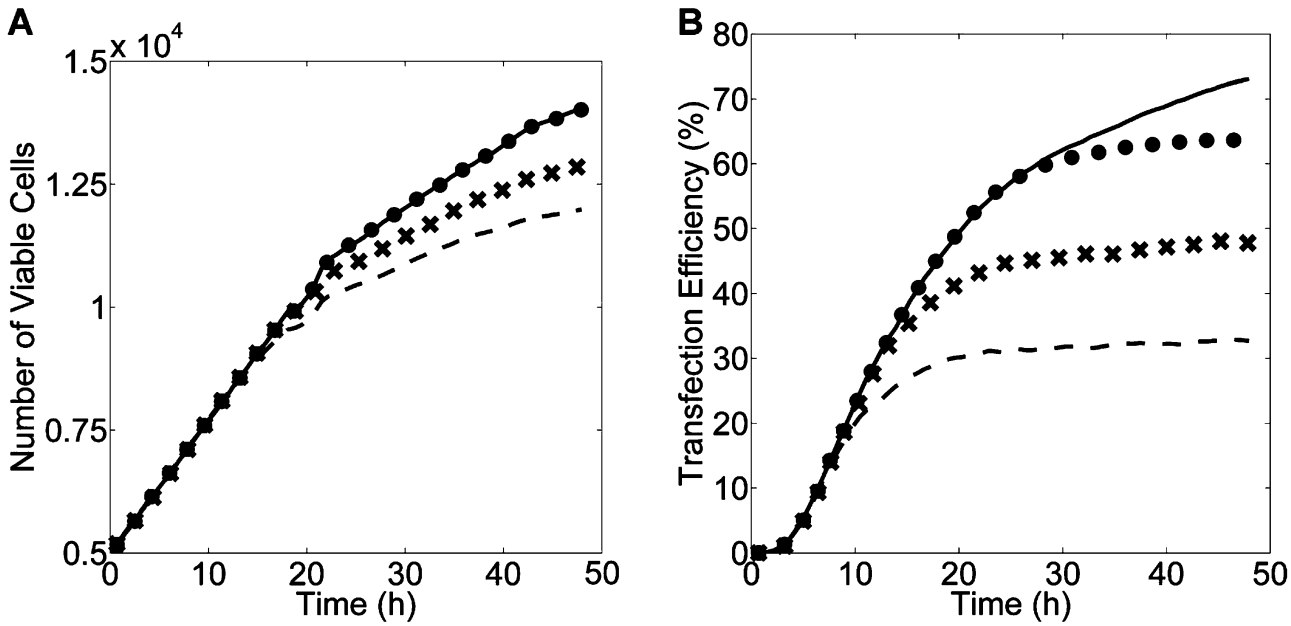

Figure 5. Toxicity threshold effect on cell viability and transfection. Output from model simulations are shown after the threshold of GFP toxicity-induced cell death was varied to be greater than 500 (dashed line), 1,000 (X mark), 2,000 (filled circle), or 4,000 (solid line) GFPs. Predicted cell viability (**A**) and transfection efficiency (**B**) increased as the threshold for GFP-induced toxicity increases.

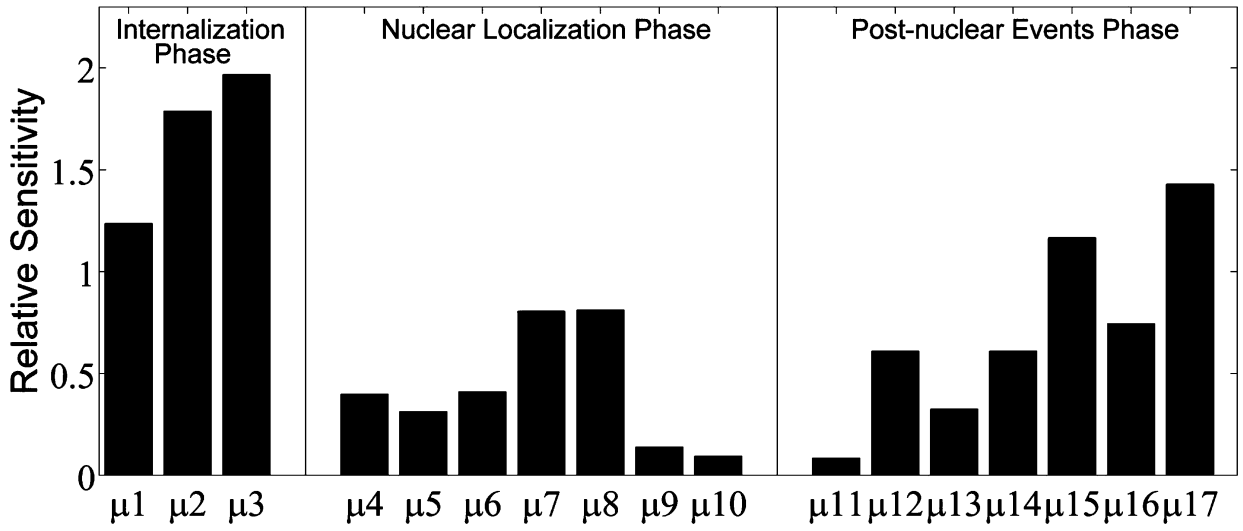

Figure 6. Sensitivity analysis. Each parameter was varied and the resulting transfection efficiencies at the 48 h time point were compared to transfection using baseline parameters (Table I; see Methods section).

results suggest that it is better to deliver a fewer number of plasmids to more cells (and therefore limit the total number of GFPs expressed per cell while keeping total transgene production high) as opposed to a larger dose to fewer cells, consistent with recommendations from another report (Moriguchi et al., 2008). Therefore, toxicity induced by overproduction of the transgene product should be considered in the design of transfection systems.

Model Parameter Sensitivity

A commonly employed technique to identify those components of the model which most affect transfection is to perform a sensitivity analysis (Saltelli et al., 2000), achieved by varying each parameter in the model and measuring the effect on the output (see Methods section). The three parameters with the largest relative sensitivity were endosomal escape $\Delta\mu_2$, lysosomal degradation $\Delta\mu_3$, and protein (matured) degradation $\Delta\mu_{17}$ with relative sensitivities of 1.79, 1.97, and 1.43, respectively (Figure 6). Endosomal escape and lysosomal degradation are believed to be a major barrier to efficient gene transfer (Wiethoff and Middaugh, 2003) and were also found to be the most sensitive of parameters in a computation model of Lipofectamine-mediated delivery of pBGal to C3A hepatocellular carcinoma cells (Varga et al., 2005). Improving endosomal escape and reducing lysosomal degradation of pDNA would result in increased cytoplasmic plasmids, an effect shown to result in increased transfection levels (Fasbender et al., 1997; Pollard et al., 1998; Tachibana et al., 2004), presumably through eventual increases in nuclear plasmids (James and Giorgio, 2000); such a process may be pDNA carrier- (Pollard et al., 1998) or cell type- dependent (Hyvonen et al., 2012). Degradation of the folded transgene product was also a sensitive parameter (Figure 6) and provides a target for improved transfection. Post-nuclear processing of the pDNA that might unfavorably affect transgene expression has recently become an important consideration in the design of the transfection system (Hama et al., 2007; Hyvonen et al., 2012; Jacobsen et al., 2009; Tachibana et al., 2004). The effect of this parameter on transfection may be explained by reports showing activation of HSP70B′, a molecular chaperone involved in protein folding and stability, to result in enhanced transfection by several fold (Martin et al., 2013; Plautz et al., 2011). Alternatively, an excess of unfolded proteins will activate the unfolded protein response (UPR), potentially leading to toxicity-induced cell death (Lee et al., 2003), which according to our model would lead to a reduction in transfection (Figure 5B). Taken together, endosomal escape, lysosomal degradation, and transgene product degradation provide targets for enhancing transfection.

Theoretical Improvements

The model simulations, as well as these sensitivity results, offer recommendations for specific barriers that future physicochemical modifications of nanoparticle systems for nonviral gene delivery should target (or help overcome) (Blessing et al., 2001; Ogris et al., 2003). Therefore, the potentially achievable changes to the gene delivery system for the most sensitive parameters (toxicity-induced GFP threshold, endosomal escape $\Delta\mu_2$, lysosomal degradation $\Delta\mu_3$, protein (matured) degradation $\Delta\mu_{17}$) were evaluated for their effect on transfection (Figure 7). When endosomal escape kinetics were increased to 1.7×10^{-2} [similar to adenoviral kinetics (Varga et al., 2005)], transfection efficiency increased from 30% to 75%, 48 h after delivery of the complex. Similarly, decreasing lysosomal degradation to 1.7×10^{-4} [which may be accomplished through dodecylation of

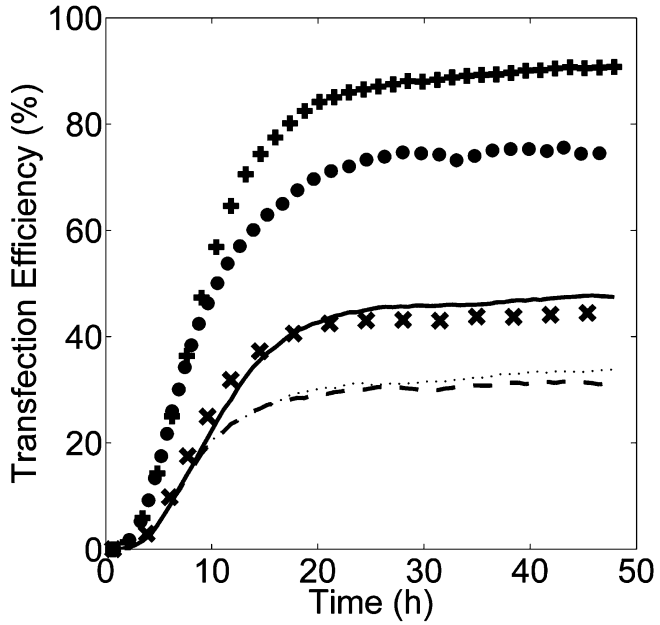

Figure 7. Theoretical improvements. Sensitive parameters of the model were varied individually and the resulting effect on transfection is shown. The combined effect of varying all of the parameters had the largest impact on transfection. Protein (matured) degradation Δ17 (dashed line), baseline (dotted line), lysosomal degradation Δ3 (X mark), toxicity-induced GFP threshold (solid line), endosomal escape Δ2 (filled circle), and combined (plus mark).

DNA carrier (Varga et al., 2005)] resulted in an increase in transfection efficiency from 30% to 40%. Decreasing protein (folded) degradation to 2.1×10^{-8} [e.g., protein mutants which stabilize conserved residues (Sacchetti et al., 2001)] resulted in no change in transfection, suggesting that this parameter alone cannot affect transfection, or an alternative improvement method is needed to fully capitalize on the parameter sensitivity to transfection, such as cell priming opposed to changes to the delivery system (Martin et al., 2013; Plautz et al., 2011). Meanwhile improving toxicity-induced threshold by twofold [e.g., reducing free DNA carrier (Godbey et al., 1999, 2001), DNA carrier coatings (Kneuer et al., 2000), or altering 5′ untranslated regions and Kozak sequences (Sacchetti et al., 2001; Sniegowski et al., 2005)] resulted in transfection increases from 30% to 45%. When all of the changes to the gene delivery system are applied in combination, the predicted transfection efficiency increases threefold, up to 90% after 24 h (Figure 7). Taken together, endosomal escape, lysosomal degradation, degradation of transgene product, and toxicity induced by transgene overproduction provide targets to engineer the gene delivery system for enhanced transfection.

Conclusions

Nonviral gene delivery systems need to be improved in order to reach therapeutically relevant levels of protein production. The design process of new gene delivery systems is quite empirical, often confounded by a design change that is an advantage to overcoming one barrier but a disadvantage to overcoming another barrier (Li et al., 2004), and the effects on pDNA routing throughout the cell remain difficult to predict. Modeling allows for easy visualization of how changes to the gene delivery system can influence subcellular distribution of pDNA, and more importantly, the effect on transgene production. Current models of gene delivery have provided valuable information, but challenges remain such as representing pDNA transfer with fuller scope and longer time frames, including those biological processes (e.g., mitosis and toxicity) that occur during longer time frames. Current models typically employ continuous and deterministic modeling methods; therefore, we present an alternative modeling technique that is discrete and stochastic, in order to open new perspectives and propose possible pathways for systematic improvement of nonviral gene delivery. Our novel application of a telecommunication model of gene delivery overcomes these challenges, describing the entire transfection process in one model, accounting for transfection up to 48 h, and including the mitosis and toxicity effect on transfection. The model can be easily adapted for other carriers by describing pDNA carrier-dependent kinetic parameters such as uptake, endosomal escape, vesicular degradation, nuclear import protein-to-vector binding, and unpackaging (Varga et al., 2005). The effect of complex type and size on internalization route or intracellular routing can also be considered [i.e., customer priority, a very important feature of queuing networks (Ross, 2000)]. The insight into the mechanisms of nonviral pDNA transfer gained from this work provides recommendations for better design of gene delivery systems that can achieve therapeutically relevant transfection levels.

References

Azzam T, Domb AJ. 2004. Current developments in gene transfection agents. Curr Drug Deliv 1(2):165–193.

Baker AH. 2004. Designing gene delivery vectors for cardiovascular gene therapy. Prog Biophys Mol Biol 84(2–3):279–299.

Banks GA, Roselli RJ, Chen R, Giorgio TD. 2003. A model for the analysis of nonviral gene therapy. Gene Ther 10(20):1766–1775.

Berraondo P, Gonzalez-Aseguinolaza G, Troconiz IF. 2009. Semi-mechanistic pharmacodynamic modelling of gene expression and silencing processes. Eur J Pharm Sci 37(3–4):418–426.

Blessing T, Kursa M, Holzhauser R, Kircheis R, Wagner E. 2001. Different strategies for formation of pegylated EGF-conjugated PEI/DNA complexes for targeted gene delivery. Bioconjug Chem 12(4):529– 537.

Boussif O, Lezoualc'h F, Zanta MA, Mergny MD, Scherman D, Demeneix B, Behr JP. 1995. A versatile vector for gene and oligonucleotide transfer into cells in culture and in vivo: polyethylenimine. Proc Natl Acad Sci USA 92(16):7297–7301.

Brunner S, Sauer T, Carotta S, Cotten M, Saltik M, Wagner E. 2000. Cell cycle dependence of gene transfer by lipoplex, polyplex and recombinant adenovirus. Gene Ther 7(5):401–407.

Candiani G, Pezzoli D, Ciani L, Chiesa R, Ristori S. 2010. Bioreducible liposomes for gene delivery: From the formulation to the mechanism of action. PLoS ONE 5(10):e13430.

Cinelli RA, Ferrari A, Pellegrini V, Tyagi M, Giacca M, Beltram F. 2000. The enhanced green fluorescent protein as a tool for the analysis of protein dynamics and localization: Local fluorescence study at the single-molecule level. Photochem Photobiol 71(6):771–776.

Cohen RN, van der Aa MA, Macaraeg N, Lee AP, Szoka FC, Jr. 2009. Quantification of plasmid DNA copies in the nucleus after lipoplex and polyplex transfection. J Control Release 135(2):166–174.

Dean DA, Dean BS, Muller S, Smith LC. 1999. Sequence requirements for plasmid nuclear import. Exp Cell Res 253(2):713–722.

Dinh AT, Pangarkar C, Theofanous T, Mitragotri S. 2007. Understanding intracellular transport processes pertinent to synthetic gene delivery via stochastic simulations and sensitivity analyses. Biophys J 92(3): 831–846.

Fasbender A, Marshall J, Moninger TO, Grunst T, Cheng S, Welsh MJ. 1997. Effect of co-lipids in enhancing cationic lipid-mediated gene transfer in vitro and in vivo. Gene Ther 4(7):716–725.

Fisher J, Henzinger TA. 2007. Executable cell biology. Nat Biotechnol 25(11):1239–1249.

Gasiorowski JZ, Dean DA. 2005. Postmitotic nuclear retention of episomal plasmids is altered by DNA labeling and detection methods. Mol Ther 12(3):460–467.

Godbey WT, Wu KK, Mikos AG. 1999. Poly(ethylenimine) and its role in gene delivery. J Control Release 60(2–3):149–160.

Godbey WT, Wu KK, Mikos AG. 2001. Poly(ethylenimine)-mediated gene delivery affects endothelial cell function and viability. Biomaterials 22(5):471–480.

Guo X, Huang L. 2012. Recent advances in nonviral vectors for gene delivery. Acc Chem Res 45(7):971–979.

Hagstrom JE. 2000. Self-assembling complexes for in vivo gene delivery. Curr Opin Mol Ther 2(2):143–149.

Hakamada K, Miyake J. 2012. Evaluation method for gene transfection by using the period of onset of gene expression and cell division. J Biosci Bioeng 113(1):124–127.

Hama S, Akita H, Iida S, Mizuguchi H, Harashima H. 2007. Quantitative and mechanism-based investigation of post-nuclear delivery events between adenovirus and lipoplex. Nucleic Acids Res 35(5):1533–1543.

He CX, Tabata Y, Gao JQ. 2010. Non-viral gene delivery carrier and its three-dimensional transfection system. Int J Pharm 386(1–2):232–242.

Horobin RW, Weissig V. 2005. A QSAR-modeling perspective on cationic transfection lipids. 1. Predicting efficiency and understanding mechanisms. J Gene Med 7(8):1023–1034.

Hume DA. 2000. Probability in transcriptional regulation and its implications for leukocyte differentiation and inducible gene expression. Blood 96(7):2323–2328.

Hyvonen Z, Hamalainen V, Ruponen M, Lucas B, Rejman J, Vercauteren D, Demeester J, De Smedt S, Braeckmans K. 2012. Elucidating the pre- and post-nuclear intracellular processing of 1,4-dihydropyridine based gene delivery carriers. J Control Release 162(1):167–175.

Jacobsen L, Calvin S, Lobenhofer E. 2009. Transcriptional effects of transfection: The potential for misinterpretation of gene expression data generated from transiently transfected cells. Biotechniques 47(1): 617–624.

James MB, Giorgio TD. 2000. Nuclear-associated plasmid, but not cell-associated plasmid, is correlated with transgene expression in cultured mammalian cells. Mol Ther 1(4):339–346.

Jandt U, Shao S, Wirth M, Zeng AP. 2011. Spatiotemporal modeling and analysis of transient gene delivery. Biotechnol Bioeng 108(9):2205–2217.

Jewett MC, Miller ML, Chen Y, Swartz JR. 2009. Continued protein synthesis at low [ATP] and [GTP] enables cell adaptation during energy limitation. J Bacteriol 191(3):1083–1091.

Kendall DG. 1953. Stochastic processes occurring in the theory of queues and their analysis by the method of the imbedded Markov chain. Ann Math Stat 24(3):338–354.

Khalil IA, Kogure K, Akita H, Harashima H. 2006. Uptake pathways and subsequent intracellular trafficking in nonviral gene delivery. Pharmacol Rev 58(1):32–45.

Klumpp S. 2011. Growth-rate dependence reveals design principles of plasmid copy number control. PLoS ONE 6(5):e20403.

Kneuer C, Sameti M, Bakowsky U, Schiestel T, Schirra H, Schmidt H, Lehr CM. 2000. A nonviral DNA delivery system based on surface modified silica-nanoparticles can efficiently transfect cells in vitro. Bioconjug Chem 11(6):926–932.

Lappalainen K, Miettinen R, Kellokoski J, Jaaskelainen I, Syrjanen S. 1997. Intracellular distribution of oligonucleotides delivered by cationic liposomes: light and electron microscopic study. J Histochem Cytochem 45(2):265–274.

Lechardeur D, Sohn KJ, Haardt M, Joshi PB, Monck M, Graham RW, Beatty B, Squire J, O'Brodovich H, Lukacs GL. 1999. Metabolic instability of plasmid DNA in the cytosol: A potential barrier to gene transfer. Gene Ther 6(4):482–497.

Ledley TS, Ledley FD. 1994.Multicompartment, numerical model of cellular events in the pharmacokinetics of gene therapies. Hum Gene Ther 5(6):679–691.

Lee AH, Iwakoshi NN, Anderson KC, Glimcher LH. 2003. Proteasome inhibitors disrupt the unfolded protein response in myeloma cells. Proc Natl Acad Sci USA 100(17):9946–9951.

Li W, Ishida T, Tachibana R, Almofti MR,Wang X, Kiwada H. 2004. Cell type-specific gene expression, mediated by TFL-3, a cationic liposomal vector, is controlled by a post-transcription process of delivered plasmid DNA. Int J Pharm 276(1–2):67–74.

Lu H, Lv L, Dai Y, Wu G, Zhao H, Zhang F. 2013. Porous chitosan scaffolds with embedded hyaluronic acid/chitosan/plasmid-DNA nanoparticles encoding TGF-beta1 induce DNA controlled release, transfected chondrocytes, and promoted cell proliferation. PLoS ONE 8(7):e69950.

Ludtke JJ, Sebestyen MG, Wolff JA. 2002. The effect of cell division on the cellular dynamics of microinjected DNA and dextran. Mol Ther 5(5 Pt 1):579–588.

Lv H, Zhang S, Wang B, Cui S, Yan J. 2006. Toxicity of cationic lipids and cationic polymers in gene delivery. J Control Release 114(1):100–109.

Martin TM, Plautz SA, Pannier AK. 2013. Network analysis of endogenous gene expression profiles after polyethyleneimine-mediated DNA delivery. J Gene Med 15(3–4):142–154.

Medina-Kauwe LK, Xie J, Hamm-Alvarez S. 2005. Intracellular trafficking of nonviral vectors. Gene Ther 12(24):1734–1751.

Mokhtari A, Christopher Frey H, Zheng J. 2006. Evaluation and recommendation of sensitivity analysis methods for application to stochastic human exposure and dose simulation models. J Expo Sci Environ Epidemiol 16(6):491–506.

Moriguchi R, Kogure K, Harashima H. 2008.Non-linear pharmacodynamics in the transfection efficiency of a non-viral gene delivery system. Int J Pharm 363(1–2):192–198.

Moroianu J, Blobel G, Radu A. 1996. Nuclear protein import: Ran-GTP dissociates the karyopherin alphabeta heterodimer by displacing alpha from an overlapping binding site on beta. Proc Natl Acad Sci USA 93(14):7059–7062.

Muller OJ, Katus HA, Bekeredjian R. 2007. Targeting the heart with gene therapy-optimized gene delivery methods. Cardiovasc Res 73(3): 453–462.

Neuts MF, Chen SZ, PULIDO Statistics. 1970. The infinite server queue with poisson arrivals and semi-markovian services. Purdue University Department of Statistics: Defense Technical Information Center.

Niidome T, Huang L. 2002. Gene therapy progress and prospects: Nonviral vectors. Gene Ther 9(24):1647–1652.

Nishikawa M, Huang L. 2001. Nonviral vectors in the new millennium: Delivery barriers in gene transfer. Hum Gene Ther 12(8):861–870.

Ogris M, Walker G, Blessing T, Kircheis R, Wolschek M, Wagner E. 2003. Tumor-targeted gene therapy: Strategies for the preparation of ligand-polyethylene glycol-polyethylenimine/DNA complexes. J Control Release 91(1–2):173–181.

Pannier AK, Ariazi EA, Bellis AD, Bengali Z, Jordan VC, Shea LD. 2007. Bioluminescence imaging for assessment and normalization in transfected cell arrays. Biotechnol Bioeng 98(2):486–497.

Parra-Guillen ZP, Gonzalez-Aseguinolaza G, Berraondo P, Troconiz IF. 2010. Gene therapy: A pharmacokinetic/pharmacodynamic modelling overview. Pharm Res 27(8):1487–1497.

Plautz SA, Boanca G, Riethoven JJ, Pannier AK. 2011. Microarray analysis of gene expression profiles in cells transfected with nonviral vectors. Mol Ther 19(12):2144–2151.

Pollard H, Remy JS, Loussouarn G, Demolombe S, Behr JP, Escande D. 1998. Polyethylenimine but not cationic lipids promotes transgene delivery to the nucleus in mammalian cells. J Biol Chem 273(13):7507–7511.

Rehman ZU, Hoekstra D, Zuhorn IS. 2013. Mechanism of Polyplex- and Lipoplex-Mediated Delivery of Nucleic Acids: Real-Time Visualization of Transient Membrane Destabilization without Endosomal Lysis. ACS Nano 7(5):3767–3777.

Ross SM. 2000. Introduction to probability models. Vol. xv. San Diego, CA: Harcourt/Academic Press. p 693. Roth CM, Sundaram S. 2004. Engineering synthetic vectors for improved DNA delivery: Insights from intracellular pathways. Annu Rev Biomed Eng 6:397–426.

Sacchetti A, El Sewedy T, Nasr AF, Alberti S. 2001. Efficient GFP mutations profoundly affect mRNA transcription and translation rates. FEBS Lett 492(1–2):151–155.

Saltelli A, Tarantola S, Campolongo F. 2000. Sensitivity analysis as an ingredient of modeling. Stat Sci 15(4):377–395.

Schwake G, Youssef S, Kuhr JT, Gude S, David MP, Mendoza E, Frey E, Radler JO. 2010. Predictive modeling of non-viral gene transfer. Biotechnol Bioeng 105(4):805–813.

Schweikl H, Hiller KA, Eckhardt A, Bolay C, Spagnuolo G, Stempfl T, Schmalz G. 2008. Differential gene expression involved in oxidative stress response caused by triethylene glycol dimethacrylate. Biomaterials 29(10):1377–1387.

Sharp AT, Pannier AK, Wysocki BJ, Wysocki TA. 2012. A novel telecommunications- based approach to HIV modeling and simulation. Nano Commun Netw 3(2):129–137.

Smith AE, Helenius A. 2004. How viruses enter animal cells. Science 304(5668):237–242.

Sniegowski JA, Lappe JW, Patel HN, Huffman HA, Wachter RM. 2005. Base catalysis of chromophore formation in Arg96 and Glu222 variants of green fluorescent protein. J Biol Chem 280(28):26248–26255.

Stallings W. 2007. Data and computer communications. Vol. xviii. Upper Saddle River, NJ: Pearson/Prentice Hall. p 878.

Tachibana R, Ide N, Shinohara Y, Harashima H, Hunt CA, Kiwada H. 2004. An assessment of relative transcriptional availability from nonviral vectors. Int J Pharm 270(1–2):315–321.

Varga CM, Hong K, Lauffenburger DA. 2001. Quantitative analysis of synthetic gene delivery vector design properties. Mol Ther 4(5):438–446.

Varga CM, Tedford NC, Thomas M, Klibanov AM, Griffith LG, Lauffenburger DA. 2005. Quantitative comparison of polyethylenimine formulations and adenoviral vectors in terms of intracellular gene delivery processes. Gene Ther 12(13):1023–1032.

Wiethoff CM, Middaugh CR. 2003. Barriers to nonviral gene delivery. J Pharm Sci 92(2):203–217.

Wilson GL, Dean BS, Wang G, Dean DA. 1999. Nuclear import of plasmid DNA in digitonin-permeabilized cells requires both cytoplasmic factors and specific DNA sequences. J Biol Chem 274(31):22025–22032.

Wysocki BJ, Martin TM, Wysocki TA, Pannier AK. 2013. Modeling nonviral gene delivery as a macro-to-nano communication system. Nano Communication Networks 4(1):14–22.

Zelphati O, Szoka FC, Jr. 1996. Mechanism of oligonucleotide release from cationic liposomes. Proc Natl Acad Sci USA 93(21):11493–11498.

Ziemer RE, Tranter WH, Fannin DR. 1998. Signals and systems: Continuous and discrete. Vol. xvii. Upper Saddle River, NJ: Prentice Hall p 622.

Zilberman M, Kraitzer A, Grinberg O, Elsner JJ. 2010. Drug-eluting medical implants. Handb Exp Pharmacol 197:299–341.

Supporting Information — Additional supporting information follows.

SUPPORTING INFORMATION FOR

Integrating Mitosis, Toxicity, and Transgene Expression in a Telecommunications Packet-Switched Network Model of Lipoplex-Mediated Gene Delivery

Timothy M. Martin[1], Beata J. Wysocki[2], Jared P. Beyersdorf[1] Tadeusz A. Wysocki[2], Angela K. Pannier[1,*]

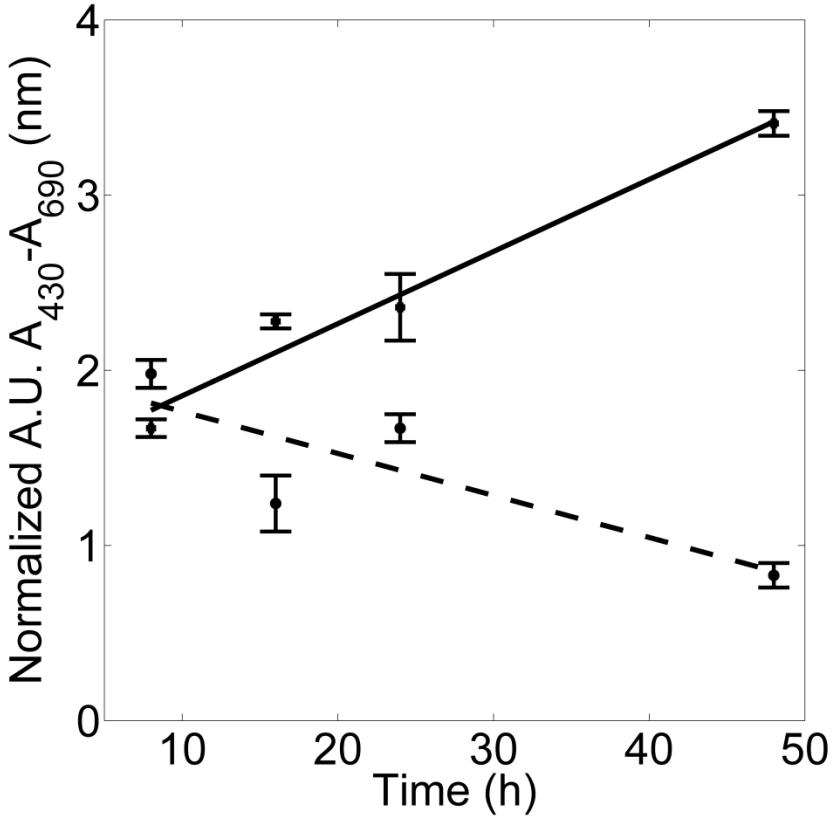

Figure S1 Toxicity induced by lipoplexes. HeLa cells were treated with lipoplexes (circles) and at the indicated time points colorimetric measurements for cell proliferation and cell viability were taken. Control cells (squares) were not treated with lipoplexes. A linear regression was fitted to the data points for treated (dashed line; $y = -0.024x + 2.0056$, $R^2 = 0.69$) and control (solid line; $y = 0.0412x + 1.4428$, $R^2 = 0.97$) measurements. The slope of each line was used to adjust rate of mitosis and toxicity threshold in model simulations (see Theoretical Aspects). Data are reported as the mean ± SEM (n = 3 for control; n = 6 for treated).